

# Guidelines for Ferroelectric FET Reliability Optimization: Charge Matching

Shan Deng, *Student Member, IEEE*, Zhan Liu, *Student Member, IEEE*, Xueqing Li, *Member, IEEE*, T. P. Ma, *Life Fellow, IEEE*, and Kai Ni, *Member, IEEE*

**Abstract**—An optimization principle for ferroelectric FET (FeFET), centered around charge matching between the ferroelectric and its underlying semiconductor, is theoretically investigated. This letter shows that, by properly reducing the ferroelectric polarization charge and its background dielectric constant, charge matching can be improved to

enable simultaneously: i) reduction of the interlayer and semiconductor electric fields during programming, reading, and retention, leading to prolonged endurance and reten-

tion; ii) improvement of the memory window; and iii) suppression of device-to-device variations by affording full polarization switching. These attributes provide an incentive for the presentation of the proposed guidelines for FeFET optimization as detailed in this letter.

**Index Terms**—Ferroelectric, FeFET, reliability optimization, charge matching.

## I. INTRODUCTION

FERROELECTRIC memory has received a strong resurgence of interest since the discovery of scalable and CMOS-compatible ferroelectrics based on HfO<sub>2</sub>. Excellent performance (e.g., more than 1 V memory window for ~10 nm thick HfO<sub>2</sub>, write time as short as 10 ns, and ultralow write energy on the order of 10 fJ, etc.) has been demonstrated in advanced technology nodes [1], [2]. However, challenges in reliability remains a major roadblock for its adoption, such as charge trapping [3], [4], degraded endurance [5], and unacceptable variations upon scaling [2], [6]. Therefore, optimization of device reliability without degrading other performance metrics will be critical for its success.

We believe that many of the reliability issues are associated with the large charge mismatch between the ferroelectric layer and the semiconductor. With the typical polarization charge around  $20 \mu\text{C}/\text{cm}^2$  for HfO<sub>2</sub>, compared with the corresponding charge on the silicon side (including the depletion charge and the channel inversion charge) of less than  $2 \mu\text{C}/\text{cm}^2$ , there is a large charge mismatch between the two, as illustrated

Manuscript received July 8, 2020; accepted July 19, 2020. Date of publication July 21, 2020; date of current version August 26, 2020. The work of Zhan Liu and T. P. Ma was supported by the NSF under Award 1941316. The review of this letter was arranged by Editor D. Ha. (Corresponding author: Kai Ni.)

Shan Deng and Kai Ni are with the Department of Microsystems Engineering, Rochester Institute of Technology, Rochester, NY 14623 USA (e-mail: kai.ni@rit.edu).

Zhan Liu and T. P. Ma are with the Department of Electrical Engineering, Yale University, New Haven, CT 06520 USA.

Xueqing Li is with the Department of Electrical Engineering Tsinghua University, Beijing 100084, China.

Color versions of one or more of the figures in this letter are available online at <http://ieeexplore.ieee.org>.

Digital Object Identifier 10.1109/LED.2020.3011037

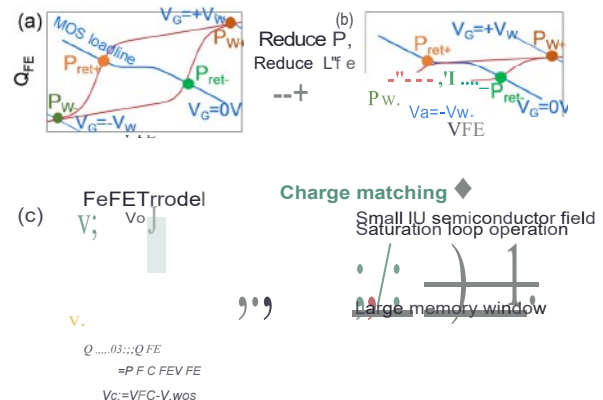


Fig. 1. Overview of charge mismatch between the ferroelectric and semiconductor, and the mitigation strategy. (a) For a normal HfO<sub>2</sub>-based FeFET with large  $P_r$  and  $\epsilon_{FE}$ , the large polarization charge ( $P_w$ ) during programming significantly stresses the interlayer and semiconductor. The blue line is the MOS loadline and the red curve is the ferroelectric  $Q_{FE}$ - $V_{FE}$  loop. (b) Reduced  $P_r$  and  $\epsilon_{FE}$  limit the switched polarization charge, and enable full polarization switching without stress on the interlayer and semiconductor. (c) The model that is utilized to investigate the optimization guidelines of FeFET.

in Fig. 1 (a). This stresses the semiconductor and interlayer significantly during programming with  $V_a = +V_w$  /  $-V_w$ , because a large polarization charge,  $P_w$  /  $-P_w$ , has to be screened by the semiconductor. Hence, substantial charge trapping and defect generation are induced by the write pulses, degrading FeFET endurance [3]. The charge mismatch also forces the ferroelectric to work on non-saturated hysteresis loops [7]. It has been shown that partial polarization switching induces significant variations due to the stochasticity during domain switching [6]. Therefore, mitigating charge mismatch becomes critical for reliability improvement.

There have been several device designs that are targeted at addressing this charge mismatch, such as FeMFET (or MF-MIS) structure [8]–[10]. In those devices, a metal-ferroelectric-metal (MFM) capacitor is integrated on top of the gate of a MOSFET. By scaling down the area of the MFM capacitor with respect to the MOSFET, the electric field in the MOSFET is reduced, and the ferroelectric can operate along the saturation loop. Challenges with this approach are the small area ratio (e.g., ~0.1) required, which limits the device scaling capability as well as retention degradation due to leakage current and depolarization field. Therefore, other approaches to improve charge matching without compromising performance are desirable.

In this work, we demonstrate an alternative approach for optimization, i.e., to reduce the ferroelectric polarization ( $P_r$ ) and its background dielectric constant ( $\epsilon_{FE}$ ) [11], [12],



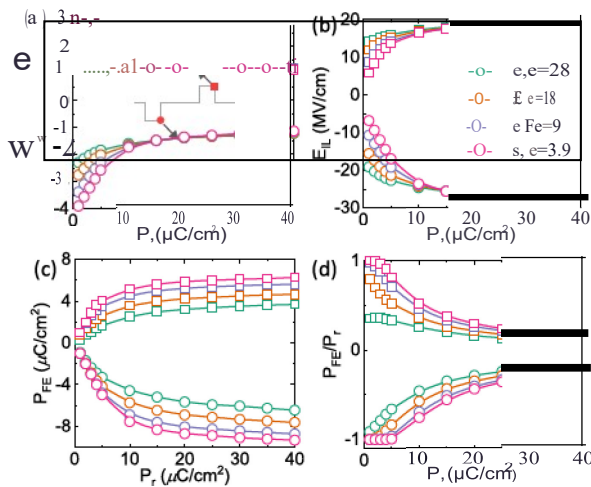


**Fig. 2.** Electric fields in (a) ferroelectrics ( $E_{FE}$ ), (b) interlayers ( $E_{IL}$ ), (c) absolute PFEs, and (d) normalized PFE/P<sub>r</sub> at the end of write pulse for 4 different dielectric constants. The square/circle symbol represents 1 $\mu$ s, +4V/-4V write pulse, respectively. All the line colors are consistent with (b).

as shown in Fig. 1 (b). In doing so, the amount of polarization that needs to be screened by the semiconductor is reduced, relieving the electrical stress in interlayer and semiconductor during programming, and thus improving the endurance, as also proposed in [13]. Additionally, it also enables the ferroelectric to operate along the saturation loop that minimizes the variation [6].

#### 11. EVALUATION APPROACH

A recently developed model for FeFET [14] is utilized to theoretically study the optimization strategy. The ferroelectric is modeled as a lumped capacitor, which is connected with the gate of a MOSFET. The voltage division equation and charge

conservation equation are solved self-consistently to obtain the

FeFET characteristics, as shown in Fig. 1 (c). The ferroelectric film is composed of multiple independent switching domains, where each domain can be in the up or down polarization state. A nucleation limited switching model is applied to describe the polarization switching dynamics [15]. With this model, the size scaling, inter-device variation, switching stochasticity, and polarization accumulation can be successfully captured.

### III. RESULTS AND DISCUSSIONS

Write pulses of  $\pm 4V$ , 1 $\mu$ s are applied to FeFETs with 8nm Hf(h as the ferroelectric and 1nm Si(h as the interlayer. The electric fields in the ferroelectrics ( $E_{FE}$ ) and interlayers ( $E_{IL}$ ) at the end of write pulses as functions of  $P_r$  with four different  $\epsilon_{FE}$  are shown in Figs. 2(a) and (b), respectively. At a given  $\epsilon_{FE}$ , the less the polarization charge that needs to be screened, the smaller the  $E_{JL}$ . This is consistent with the charge conservation requirement (Fig. 1 (c)). A smaller  $P_r$  improves the charge matching between the ferroelectric and the semiconductor, relieving the electrical stress on the interlayer and semiconductor. Moreover, additional drop in  $E_{IL}$  can be achieved by lowering  $\epsilon_{FE}$ . For example, during the -4V write pulse,  $E_{IL}$  reduces merely 1.3x when  $P_r$  shrinks from 20 $\mu C/cm^2$  to 2 $\mu C/cm^2$  for  $\epsilon_{FE} = 28$ ; while reduces as much as 2x for  $\epsilon_{FE} = 9$ . Such decline in  $E_{IL}$  is beneficial for

endurance improvement, as it can reduce charge trapping and interface defect generation.

The boost of  $E_{FE}$  is a direct consequence of the reduction in  $E_{JL}$ . As such, the  $E_{FE}$  increases by 1.7x when  $P_r$  shrinks from 20 $\mu C/cm^2$  to 2 $\mu C/cm^2$  for  $\epsilon_{FE} = 28$ , and grows by 2.5x for  $\epsilon_{FE} = 9$ . Note that this  $E_{FE}$  increase should not degrade the endurance of the Hf(h-based FeFET ( $\sim 10^5$  cycles [1], [2]), as it is mainly limited by charge trapping [5]. This is further illustrated by the much higher endurance ( $> 10^8$  cycles [16], [17]) in MFM capacitors cycled with similar  $E_{FE}$  stress ( $E_{FE} \sim 3MV/cm$ ). The absolute and normalized polarization charge (PFE) at the end of write pulses are shown in Figs. 2(c) and (d), respectively. The enhancement in switched PFE with  $P_r$  becomes marginal when  $P_r$  grows beyond 15 $\mu C/cm^2$ . This indicates that, for the optimization of FeFET, pursuing a high  $P_r$  is the wrong direction because: (i) it will not improve the switched PFE, and even worse, (ii) it will increase the stress on the interlayer and semiconductor, degrading its reliability. The normalized PFE indicates the portion of domains that participate in the switching process. Interestingly, it exhibits an opposite trend to the absolute PFE due to the saturating behavior of PFE with respect to  $P_r$ . For small  $P_r$ , especially at small  $\epsilon_{FE}$ , the  $PFE/P_r$  is close to 1, indicating full polarization switching due to the charge matching. The benefit of full polarization switching in controlling the variation will be explained below.

When the applied gate pulse is turned off, some of the switched domains will flip back, relaxing the polarization. Fig. 3(a) shows that PFE during retention exhibits a peak at some intermediate  $P_r$ , especially for small  $\epsilon_{FE}$ . This is related to the depolarization field [18], shown in Eq. 1, that causes the polarization relaxation.

$$V_{FE,ret} = - \frac{PFE}{C_{FE} + C_{1s}} \quad (1)$$

where  $V_{FE,ret}$  is the voltage across the ferroelectric during retention,  $C_{1s}$  is the series combination of the interlayer and the semiconductor capacitance. As shown in Fig. 3(c), the depolarization field at the initial relaxation moment strengthens with increasing  $P_r$ , and get further enhanced for small  $E_{FE}$ , which is consistent with Eq. (1). For small  $P_r$ , the depolarization field is sufficiently small such that PFE during retention follows the switched  $E_{FE}$  after the write pulse (Fig. 2(c)). However, for a large  $P_r$ , the depolarization field is strong enough to cause significant polarization relaxation after the write pulse, causing the decline of  $E_{FE}$ . This is also illustrated in the transient waveform for a -4V write pulse, shown in Fig. 3(e). At the moment when  $V_a$  switches from -4V to 0V, the  $V_{FE,ret}$  is greater for higher  $P_r$ , causing more polarization relaxation. As a result, a nonmonotonic dependence is observed. Note that even after polarization relaxation, shown in Fig. 3(a), nearly full polarization switching is observed for small  $P_r$  and  $E_{FE}$ , suggesting its potential for suppressing inter-device variations.

According to Eq.(1), there is a tradeoff between the memory window and depolarization field, hence retention performance. The depolarization field during retention, shown in Fig. 3(b) follows a similar trend as the Fig. 3(a), due to Eq. (1).

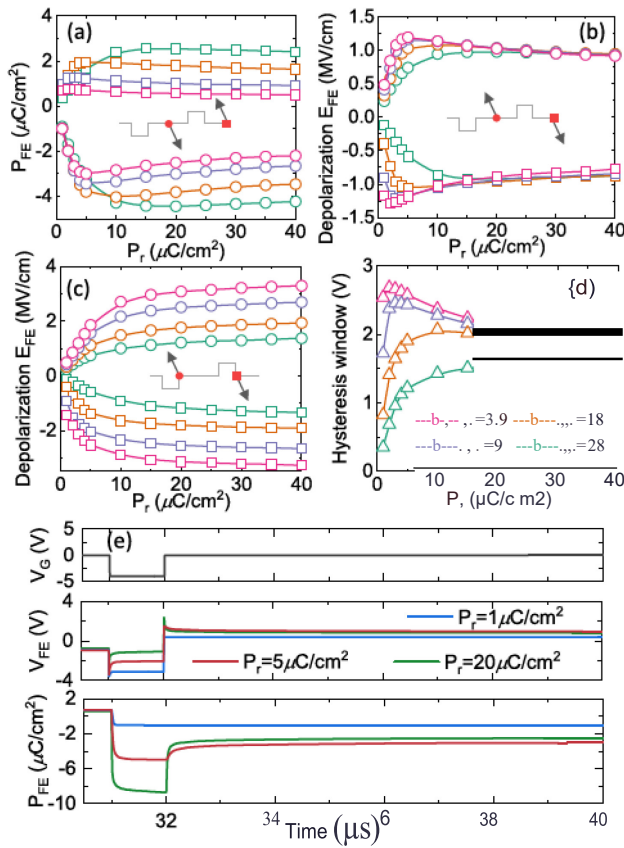


Fig. 3. (a) PFE and (b) the depolarization field EFE during retention; (c) The depolarization field EFE at the initial relaxation moment; (d) Memory windows of FeFET as functions of  $P_r$  for 4 different  $eFE$ ; (e) transient waveforms showing polarization switching and relaxation during -4V writepulse for 3 different  $P_r$  cases. The square/circle symbol in (a-c) represents 1μs, +4V/-4V write pulse, respectively. Curve colors are consistent with (d).

It suggests that even though the depolarization field at the initial relaxation moment (Fig. 3(c)) is much higher for a film with a smaller  $eFE$ , it does not hold for the depolarization field during retention. This is because PFE during retention is also reduced for small  $eFE$ , thus rendering similar depolarization field during retention, irrespective of the  $eFE$ . For example, for a  $eFE$  of 9, the  $EFE$  during retention increases approximately only 30% when  $P_r$  reduces from 25μC/cm² to 5μC/cm² (the peak of the curve). It is also possible to maintain the same depolarization field as the existing HfO2 FeFET ( $P_r$  of 20 μC/cm² and  $eFE$  of 28) by simultaneously decreasing  $P_r$  and  $eFE$ . Therefore, it is still possible to improve the device reliability, including retention, while maintaining the same device performance.

Fig. 3(d) shows the FeFET memory windows as functions of  $P_r$  for four different  $eFE$ . It suggests that the degradation in memory window caused by weak  $P_r$  can be compensated by reducing  $eFE$ . This again demonstrates that pursuing a high  $P_r$  is not the right direction as only marginal improvement in memory window can be achieved given the limited write voltage. Thus, the FeFET reliability can be improved without degrading its performance.

The simulated device-to-device variations in scaled FeFET are presented in Fig. 4. The model incorporates a Monte Carlo

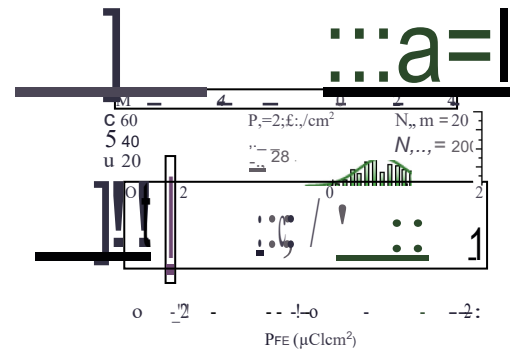


Fig. 4. Device-to-device variations of FeFETs with 3 different  $P_r$  and  $eFE$  combinations. The distributions of PFE after +4V and -4V write pulses are shown. 200 devices each with 20 domains are simulated.

induced by the switching process [14]. For a FeFET with  $P_r$  of 20μC/cm² and  $eFE$  of 28, only 20% of domains participate

in the switching. Reducing  $P_r$  to 2μC/cm increases  $EFE$  framework, which allows to capture the intrinsic variations

during write, resulting in nearly full polarization switching. Reducing  $eFE$  to 9 further suppresses the variation. This suggests that, by proper charge matching between the ferroelectric and the semiconductor,  $EFE$  can be enhanced to enable full polarization switching, regardless of the ferroelectric domain distribution. This could potentially provide a way to suppress the variations. Note that this model only captures the lower bound of the variation as it only considers variation induced by the intrinsic ferroelectric switching process without taking into account the phase inhomogeneity [19] and sources for conventional transistor variations [20]. The appropriate design of relatively low  $Pr$  and  $EFE$  ferroelectrics compared to the prevailing values currently being pursued, should therefore be the target for the optimization of FeFETs for memory applications.

Engineering a HfO<sub>2</sub> based ferroelectric film with low  $Pr$  and  $eFE$  should therefore be the target for the optimization of FeFET. Previously, a polarization reduction strategy has been proposed, which is to control the polarization orientation so that the out of plane polarization component can be reduced [13]. However, its effectiveness remains to be tested. Moreover, several other strategies can also be potentially applied. For example, it has been shown that by inhomogeneous layering of HfO<sub>2</sub> and SiO<sub>2</sub>, the remnant polarization and potentially also the dielectric constant can be reduced [21]. Another interesting approach to reduce  $Pr$  and  $eFE$  is through film engineering by adjusting the atomic layer deposition cycle ratio of HfO<sub>2</sub> and ZrO<sub>2</sub> [22]. Therefore, exploration in the processing techniques and their effectiveness in reducing  $Pr$  and  $EFE$ , and thus improvement in FeFET reliability, will need to be performed in the future.

#### IV. CONCLUSION

Based on the simple principle of proper charge matching between the ferroelectric and its underlying semiconductor, we have presented a set of guidelines for optimizing HfO<sub>2</sub>-based FeFETs for nonvolatile memory applications. Specifically, our simulation results have demonstrated that, by appropriately reducing the ferroelectric's  $Pr$  and its background  $EFE$ , the electrical stress in the inter-layer/semiconductor can be reduced, the memory window can be improved, and the inter-device variations can be suppressed.



## REFERENCES

- [1] M. Trentzsch, S. Flachowsky, R. Richter, J. Paul, B. Reimer, D. Utes, S. Jansen, H. Mulaosmanovic, S. Müller, S. Slesazek, J. Ocker, M. Noack, J. Müller, P. Polakowski, J. Schreiter, S. Beyer, T. Mikolajick and B. Rice, "A 28 nm HKMG super low power embedded NVM technology based on ferroelectric FETs," in *JEDM Tech. Dig.*, Dec. 2016, pp. 294-297, doi: [10.1109/IEDM.2016.7838397](https://doi.org/10.1109/IEDM.2016.7838397).
- [2] S. Dunke, I. M. Trentzsch, R. Richter, P. Moll, C. Fuchs, O. Gehring, M. Majer, S. Wittek, B. Müller, T. Melde, H. Mulaosmanovic, S. Slesazek, S. Müller, J. Ocker, M. Noack, D.-A. Lohr, P. Polakowski, J. Müller, T. Mikolajick, J. Hontschel, B. Rice, J. Pellerin, and S. Beyer, "A FeFET based super-low-power ultra-fast embedded NVM technology for 22 nm FDSOI and beyond," in *JEDM Tech. Dig.*, Dec. 2017, pp. 485-488, doi: [10.1109/IEDM.2017.8268425](https://doi.org/10.1109/IEDM.2017.8268425).
- [3] K. Ni, P. Sharma, J. Zhang, M. Jerry, J. A. Smith, K. Tapily, R. Clark, S. Mahapatra, and S. Datta, "Critical role of interlayer in Hf<sub>0.5</sub>Zr<sub>0.2</sub> ferroelectric FET nonvolatile memory performance," *IEEE Trans. Electron Devices*, vol. 65, no. 6, pp. 2461-2469, Jun. 2018, doi: [10.1109/LED.2018.2829122](https://doi.org/10.1109/LED.2018.2829122).
- [4] E. Yurchuk, J. Müller, S. Müller, J. Paul, M. Pesic, R. van Bentum, U. Schroeder, and T. Mikolajick, "Charge-trapping phenomena in HfO<sub>2</sub>-based FeFET-type nonvolatile memories," *IEEE Trans. Electron Devices*, vol. 63, no. 9, pp. 3501-3507, Sep. 2016, doi: [10.1109/LED.2016.2588439](https://doi.org/10.1109/LED.2016.2588439).
- [5] E. Yurchuk, S. Mueller, D. Martin, S. Slesazek, U. Schroeder, T. Mikolajick, J. Müller, J. Paul, R. Hoffmann, J. Sundqvist, T. Schlosser, R. Boschke, R. van Bentum, and M. Trentzsch, "Origin of the endurance degradation in the novel HfO<sub>2</sub>-based IT ferroelectric non-volatile memories," in *Proc. IEEE Int. Rel. Phys. Symp.*, Jun. 2014, pp. 2E-1-2E-5, doi: [10.1109/IRPS.2014.6860603](https://doi.org/10.1109/IRPS.2014.6860603).
- [6] K. Ni, W. Chakraborty, J. Smith, B. Grisafe, and S. Datta, "Fundamental understanding and control of device-to-device variation in deeply scaled ferroelectric FETs," in *Proc. Symp. VLSI Tech 1101*, Jun. 2019, pp. 40-41, doi: [10.23919/NLSIT.2019.8776497](https://doi.org/10.23919/NLSIT.2019.8776497).
- [7] K. Ni, M. Jerry, J. A. Smith, and S. Datta, "A circuit compatible accurate compact model for ferroelectric FETs," in *Proc. IEEE Symp. VLSI Tech 1101*, Jun. 2018, pp. 131-132, doi: [10.1109/NLSIT.2018.8510622](https://doi.org/10.1109/NLSIT.2018.8510622).
- [8] K. Ni, J. A. Smith, B. Grisafe, T. Rakshit, B. Obradovic, J. A. Kitt, M. Rodder, and S. Datta, "SoC logic compatible multi-bit FeFET weight cell for neuromorphic applications," in *JEDM Tech. Dig.*, Dec. 2018, pp. 296-299, doi: [10.1109/IEDM.2018.8861446](https://doi.org/10.1109/IEDM.2018.8861446).
- [9] E. Tokumitsu, G. Fujii, and H. Ishiwara, "Electrical properties of metal-ferroelectric-insulator-semiconductor (MFIS) and metal-ferroelectric-metal-insulator-semiconductor (MFIS)-FETs using ferroelectric SrBi<sub>2</sub>Ta<sub>2</sub>O<sub>9</sub> film and SrTa<sub>2</sub>O<sub>6</sub>/SiON buffer layer," *Jpn. J. Appl. Phys.*, vol. 39, pp. 2125-2130, Apr. 2000, doi: [10.1143/JJAP.39.2125](https://doi.org/10.1143/JJAP.39.2125).
- [10] S.-J. Yoon, D.-H. Min, S.-E. Moon, K. S. Park, J. I. Won, and S.-M. Yoon, "Improvement in long-term and high-temperature retention stability of ferroelectric field-effect memory transistors with metal-ferroelectric-metal-insulator-semiconductor gate-stacks using Al<sub>2</sub>O<sub>3</sub>-doped HfO<sub>2</sub> thin films," *IEEE Trans. Electron Devices*, vol. 67, no. 2, pp. 499-504, Feb. 2020. [Online]. Available: <https://ieeexplore.ieee.org/abstract/document/8954955>
- [11] T. Li, S. T. Hsu, B. Ulrich, H. Ying, L. Stecker, D. Evans, Y. Ono, J.-S. Maa, and J. J. Lee, "Fabrication and characterization of a Pb<sub>5</sub>Ge<sub>3</sub>O<sub>11</sub> one-transistor-memory device," *Appl. Phys. Lett.*, vol. 79, no. 11, pp. 1661-1663, Sep. 2001, doi: [10.1063/1.1401092](https://doi.org/10.1063/1.1401092).
- [12] T. Li, S. T. Hsu, B. D. Ulrich, L. Stecker, D. R. Evans, and J. J. Lee, "One transistor ferroelectric memory with Pt/Ph<sub>5</sub>Ge<sub>3</sub>O<sub>11</sub>/Ir/Poly-Si/SiO<sub>2</sub>/Si gate stack," *IEEE Electron Device Lett.*, vol. 23, no. 6, pp. 339-341, Jun. 2002, doi: [10.1109/LED.2002.1004228](https://doi.org/10.1109/LED.2002.1004228).
- [13] J. Müller, P. Polakowski, S. Müller, H. Mulaosmanovic, J. Ocker, T. Mikolajick, S. Slesazek, S. Müller, J. Ocker, T. Mikolajick, S. Flachowsky, and M. Trentzsch, "High endurance strategies for hafnium oxide based ferroelectric field effect transistor," in *Proc. Non-Volatile Memory Technol. Symp. (NVMTS)*, Oct. 2016, pp. 1-7, doi: [10.1109/NVMTS.2016.7781517](https://doi.org/10.1109/NVMTS.2016.7781517).
- [14] S. Deng, G. Yin, W. Chakraborty, S. Dutta, S. Datta, X. Li, and K. Ni, "A comprehensive model for ferroelectric FET capturing the key behaviors: Scalability, variation, stochasticity, and accumulation," in *Dig. Tech. Papers-Symp. VLSI Technol.*, 2020.
- [15] C. Alessandri, P. Pandey, A. Abusleme, and A. Seabaugh, "Monte Carlo simulation of switching dynamics in polycrystalline ferroelectric capacitors," *IEEE Trans. Electron Devices*, vol. 66, no. 8, pp. 3527-3534, Aug. 2019, doi: [10.1109/TEDE.2019.2922268](https://doi.org/10.1109/TEDE.2019.2922268).
- [16] M. Peic, F. P. G. Flegler, L. Larcher, A. Padovani, T. Schenk, E. D. Grimley, X. Sang, J. M. LeBeau, S. Slesazek, U. Schroeder, and T. Mikolajick, "Physical mechanisms behind the field-cycling behavior of HfO<sub>2</sub>-based ferroelectric capacitors," *Adv. Funct. Mater.*, vol. 26, no. 25, pp. 4601-4612, Jul. 2016, doi: [10.1002/adfm.206100590](https://doi.org/10.1002/adfm.206100590).
- [17] S. Mueller, J. Müller, R. Hoffmann, E. Yurchuk, T. Schlosser, R. Boschke, J. Paul, M. Goldbach, T. Herrmann, A. Zaka, U. Schroeder, and T. Mikolajick, "From MFM capacitors toward ferroelectric transistors: Endurance and disturb characteristics of HfO<sub>2</sub>-based FeFET devices," *IEEE Trans. Electron Devices*, vol. 60, no. 12, pp. 4199-4205, Dec. 2013, doi: [10.1109/TEDE.2013.2283465](https://doi.org/10.1109/TEDE.2013.2283465).
- [18] T. P. Ma and J.-P. Han, "Why is nonvolatile ferroelectric memory field-effect transistor still elusive?" *IEEE Electron Device Lett.*, vol. 23, no. 7, pp. 386-388, Jul. 2002, doi: [10.1109/LED.2002.1015207](https://doi.org/10.1109/LED.2002.1015207).
- [19] Y.-S. Liu and P. Su, "Variability analysis for ferroelectric FET non-volatile memories considering random ferroelectric phase distribution," *IEEE Electron Device Lett.*, vol. 41, no. 3, pp. 369-372, Mar. 2020, doi: [10.1109/LED.2020.2967423](https://doi.org/10.1109/LED.2020.2967423).
- [20] K. Ni, A. Gupta, O. Prakash, S. Thomann, X. S. Hu, and H. Amrouch, "Impact of extrinsic variation sources on the device-to-device variation in ferroelectric FET," in *Proc. IEEE Int. Rel. Phys. Symp. (IRPS)*, Apr. 2020, pp. 1-5, doi: [10.1109/IRPS45951.2020.9128323](https://doi.org/10.1109/IRPS45951.2020.9128323).
- [21] P. D. Lomenzo, Q. Takmeel, C. Zhou, Y. Liu, C. M. Fancher, J. L. Jones, S. Moghaddam, and T. Nishida, "The effects of layering in ferroelectric Si-doped HfO<sub>2</sub> thin films," *Appl. Phys. Lett.*, vol. 105, no. 7, Aug. 2014, Art. no. 072906, doi: [10.1063/1.4893738](https://doi.org/10.1063/1.4893738).
- [22] J. Liao, B. Zeng, Q. Sun, Q. Chen, M. Liao, C. Qiu, Z. Zhang, and Y. Zhou, "Grain size engineering of ferroelectric Zr-doped HfO<sub>2</sub> for the highly scaled devices applications," *IEEE Electron Device Lett.*, vol. 40, no. 11, pp. 1868-1871, Nov. 2019, doi: [10.1109/LED.2019.2944491](https://doi.org/10.1109/LED.2019.2944491).